

## Model for force fluctuations in bead packs

S. N. Coppersmith,<sup>1,2</sup> C.-h. Liu,<sup>3,4</sup> S. Majumdar,<sup>5</sup> O. Narayan,<sup>6,7</sup> and T. A. Witten<sup>8</sup>

<sup>1</sup>*AT&T Bell Laboratories, Murray Hill, New Jersey 07974*

<sup>2</sup>*James Franck Institute, University of Chicago, 5640 Ellis Avenue, Chicago, Illinois 60637\**

<sup>3</sup>*Exxon Research & Engineering Company, Route 22 East, Annandale, New Jersey 08801*

<sup>4</sup>*Xerox Webster Research Center, 800 Phillips Road, Webster, New York 14580\**

<sup>5</sup>*Department of Physics, Yale University, New Haven, Connecticut 06511*

<sup>6</sup>*Department of Physics, Harvard University, Cambridge, Massachusetts 02138*

<sup>7</sup>*Department of Physics, University of California, Santa Cruz, California 95064\**

<sup>8</sup>*James Franck Institute, University of Chicago, 5640 Ellis Avenue, Chicago, Illinois 60637*

(Received 27 November 1995)

We study theoretically the complex network of forces that is responsible for the static structure and properties of granular materials. We present detailed calculations for a model in which the fluctuations in the force distribution arise because of variations in the contact angles and the constraints imposed by the force balance on each bead of the pile. We compare our results for the force distribution function for this model, including exact results for certain contact angle probability distributions, with numerical simulations of force distributions in random sphere packings. This model reproduces many aspects of the force distribution observed both in experiment and in numerical simulations of sphere packings. Our model is closely related to some that have been studied in the context of self-organized criticality. We present evidence that in the force distribution context, “critical” power-law force distributions occur only when a parameter (hidden in other interpretations) is tuned. Our numerical, mean field, and exact results all indicate that for almost all contact distributions the distribution of forces decays exponentially at large forces. [S1063-651X(96)07005-5]

PACS number(s): 02.50.Ey, 81.05.Rm

### I. INTRODUCTION

Disordered geometric packings of granular materials [1] have fascinated researchers for many years [2]. Such studies, with their applicability to the geometry of glass-forming systems, initially were concerned with categorizing the void shapes and densities. More recently, partly in recognition of the ubiquity of granular materials and their importance to a wide variety of technological processes, interest has focused on how the forces supporting the grains are distributed. Visualizations of two-dimensional granular systems [3] demonstrate weight concentration into “force chains.” It is natural to expect that similar concentrations of forces will occur in three dimensions. The distinctive forces in bead packs also give rise to distinctive boundary-layer flow [4] and novel sound-propagation properties [5].

Reference [6] presents experiments, simulations, and theory characterizing the inhomogeneous forces that occur in stationary three-dimensional bead packs, focusing particularly on the relative abundance of forces that are much larger than the average. If the bead pack were a perfect lattice, then, at any given depth, no forces would be greater than some definite multiple of the average force. At the other extreme, if the network of force-bearing contacts were fractal [7], then fluctuations in the forces (characterized, say, by their variance) would become arbitrarily large compared to the average force at a given depth, as the system size is increased. Reference [6] shows that the forces in bead packs are intermediate between these two extremes. The forces are un-

bounded, but the number of large forces falls off exponentially with the force. The fluctuations remain roughly the same as the average force, regardless of how large the bead pack becomes. A simple model was introduced to understand the results of the experiments and simulations.

This paper presents the detailed analysis of the model introduced in Ref. [6]. The model yields force distributions which agree quantitatively with those obtained in numerical simulations of sphere packings. Generic distributions of contacts lead to force distributions which decay exponentially at large forces, though a special distribution exists for which the force distribution is a power law. We discuss the relationship of this model to other related systems and present the analysis leading to the results that are quoted in Ref. [6] without derivation.

The paper is organized as follows. Section II defines the model, discusses several limiting cases that have been discussed previously in other contexts, and then presents our analysis of the force distribution expected in the context of force chains in bead packs. Special emphasis is placed on one particular contact distribution, the “uniform” distribution, which is the most random distribution consistent with the constraint of force balance. We first present a mean field solution for this model, and then show that this mean field solution is exact. We also obtain exact results for a countable set of nongeneric distributions as well as the mean field and numerical results for other contact distributions. Evidence is presented that almost all contact distributions lead to exponentially decaying force distributions. Section III discusses numerical simulations of sphere packings, which we analyze to obtain contact probability distributions to be used in the  $q$  model. We show that the force distribution predicted by the

\*Present address.

model with this contact distribution agrees quantitatively with the force distribution in the simulation. The Appendix presents some mathematical identities concerning the uniform  $q$  distribution which are used in the text.

## II. THE $q$ MODEL

### A. Definition of the model

Here we introduce the model, which assumes that the dominant physical mechanism leading to force chains is the inhomogeneity of the packing causing an unequal distribution of the weights on the beads supporting a given grain. Spatial correlations in these fractions as well as variations in the coordination numbers of the grains are ignored. We consider a regular lattice of sites, each with a particle of mass unity. Each site  $i$  in layer  $D$  is connected to exactly  $N$  sites  $j$  in layer  $D+1$ . Only the vertical components of the forces are considered explicitly (it is assumed that the effects of the horizontal forces can be absorbed in the random variables  $q_{ij}$  defined below). A fraction  $q_{ij}$  of the total weight supported by particle  $i$  in layer  $D$  is transmitted to particle  $j$  in layer  $D+1$ . Thus, the weight supported by the particle in layer  $D$  at the  $i$ th site,  $w(D,i)$ , satisfies the stochastic equation

$$w(D+1,j) = 1 + \sum_i q_{ij}(D)w(D,i). \quad (2.1)$$

We take the fractions  $q_{ij}(D)$  to be random variables, independent except for the constraint  $\sum_j q_{ij} = 1$ , which enforces the condition of force balance on each particle. We assume that the probability of realizing a given assortment of  $q$ 's at each site  $i$  is given by a distribution function  $\rho(q_{i1}, \dots, q_{iN}) = \{\prod_j f(q_{ij})\} \delta(\sum_j q_{ij} - 1)$ . We define the induced distribution  $\eta(q)$  as

$$\eta(q) = \prod_{j \neq k} \int dq_{ij} \rho(q_{i1}, \dots, q_{ik} = q, \dots, q_{iN}). \quad (2.2)$$

Because  $\rho(q_{i1}, \dots, q_{iN})$  is a probability distribution and  $\sum_{j=1}^N q_{ij} = 1$ , the induced distribution must satisfy the conditions  $\int_0^1 dq \eta(q) = 1$ ,  $\int_0^1 dq q \eta(q) = 1/N$ .

In this paper we focus on the force distribution  $Q_D(w)$ , which is the probability that a site at depth  $D$  is subject to vertical force  $w$ . We obtain  $Q_D(w)$  for different distributions of  $q$ 's. We will also consider the force distribution  $P_D(v)$  for the normalized weight variable  $v = w/D$ . For  $\eta(q) = \delta(q - 1/N)$ , where each particle distributes the vertical force acting on it equally among all its neighbors, the force distribution at a given depth is homogeneous:  $Q_D(w) = \delta(w - D)$ , or  $P_D(v) = \delta(v - 1)$ . At the other extreme, there is a ‘‘critical’’ limit, when  $q$  can only take on the values 1 or 0, so that weight is transmitted to a single underlying particle. For this, as discussed in the next section, the force distribution obeys a scaling form and decays as a power law at large forces,  $Q(w) \propto w^{-c}$ , where  $c(N \geq 3) = \frac{3}{2}$  and  $c(N = 2) = \frac{4}{3}$ . We demonstrate that this power law does not occur when  $q$  can take on values other than 1 and 0, as is the case for real packings. Generic continuous distributions of  $q$ 's lead to a distribution of weights that, normalized to the mean, is independent of depth at large  $D$  and which decays exponentially at large weights. We solve the model exactly for a countable infinite

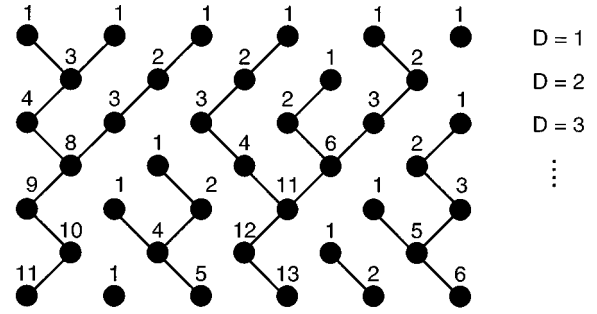


FIG. 1. Schematic diagram showing the paths of weight support for a two-dimensional system in the  $q_{0,1}$  limit where each site transmits its weight to exactly one neighbor below. The numbers at each site are the values of  $w(i,D)$ .

set of  $q$  distributions, and present mean field and numerical results for other distributions of  $q$ 's.

### B. $q$ model for the ‘‘critical’’ case

We first consider the case where each particle transmits its weight to exactly one neighbor in the layer below, so that the variable  $q$  is restricted to taking on only the values 0 and 1. We denote this (singular) limiting case of our model by the ‘‘ $q_{0,1}$  limit.’’ Figure 1 shows the paths of weight support for a two-dimensional system in this limit. The solid lines correspond to bonds for which  $q=1$ . The paths of weight support of particles in the top row are coalescing random walks. Since a random walk of length  $D$  has typical transverse excursion of  $D^{1/2}$ , for the two-dimensional case the maximum weight supported by an individual grain at depth  $D$  scales as  $D^{3/2}$  [8]. Because  $D^{3/2} \gg D$ , the mean weight supported at depth  $D$ , it is plausible that in the  $q_{0,1}$  limit the model yields a broad weight distribution.

The defining equations of the  $q_{0,1}$  limit of our model are known to be identical to those of Scheidegger’s model of river networks [9] and a model of aggregation with injection [10,11]; the model is also equivalent to that of directed Abelian sandpiles [12–14]. (The number of neighbors below a particle,  $N$ , corresponds to the dimensionality  $d$  in these models.) The last equivalence follows [13,14] if we define  $G_0(\vec{X}_1; \vec{X}_0)$  as the probability that the weight of site  $\vec{X}_1$  is supported by site  $\vec{X}_0$  in the same row or below it. The conditional probability that  $\vec{X}_1$  is supported by  $\vec{X}_0$ , given that  $l$  of the  $N$  neighboring particles in the row below are supported by  $\vec{X}_0$ , is  $l/N$ . Thus,

$$G_0(\vec{X}_1; \vec{X}_0) = \frac{1}{N} \sum_{i=1}^N G_0(\vec{X}_1 - \vec{e}_i; \vec{X}_0) + \delta_{\vec{X}_1, \vec{X}_0}, \quad (2.3)$$

where  $\{\vec{X}_1 - \vec{e}_i\}$  are the neighbors of  $\vec{X}_1$  in the row below it, and the  $\delta$ -function term follows because each particle must support its own weight. Similarly, the probability that two sites  $\vec{X}_1$  and  $\vec{X}_2$  in the same row are supported by  $\vec{X}_0$  satisfies

$$G(\vec{X}_1, \vec{X}_2; \vec{X}_0) = \frac{1}{N^2} \sum_i \sum_j G(\vec{X}_1 - \vec{e}_i, \vec{X}_2 - \vec{e}_j; \vec{X}_0) \quad (2.4)$$

for  $\vec{X}_1 \neq \vec{X}_2$ . These equations are precisely those that describe the behavior of the correlations of the avalanches in the directed Abelian sandpile [12,15]. In this model, an integer ‘‘height’’ variable  $z(\vec{X})$  is assigned each site  $\vec{X}$  on a lattice. The dynamics are defined by the rule that if any  $z(\vec{X})$  exceeds a critical value  $z_c$ , then the variables at  $m$  nearest neighbor sites along a preferred direction increase by 1, while  $z(\vec{X})$  decreases by  $m$ . In this context  $G_0(\vec{X}_1; \vec{X}_0)$  is identified with the probability that adding a particle at  $\vec{X}_0$  creates an avalanche that topples over the site  $\vec{X}_1$ . Higher order correlations are mapped similarly. The distribution of weights in our model is mapped to the distribution of avalanche sizes.

All these models [9–13] have been studied as examples of self-organized criticality [16] because they lead to power-law correlations without an obvious tuning parameter. However, in the context of our model, the  $q_{0,1}$  limit is a singular one, where the probability of  $q \neq \{0,1\}$  has been tuned to zero. As we shall show in this paper, generic distributions  $\eta(q)$ , for which the probability that  $q \neq \{0,1\}$  is nonzero (no matter how small), yield completely different results, with the distribution of weights decaying exponentially at large weights. With hindsight, we identify the probability for a river to split in the river network model [9], and the probability for a colloidal particle to fragment in the aggregation model [10,13] as hidden parameters that were tuned to zero. The corresponding parameter for directed Abelian sandpiles is less obvious.

The equivalence of our model in the  $q_{0,1}$  limit to the models discussed above can be exploited to obtain some results for the distribution of weights. Recalling that the dimensionality  $d$  in these models corresponds to our  $N$ , we know that the weight distribution function at a depth  $D$ ,  $Q_D(w)$ , has a scaling form for all  $N$ :

$$Q_D(w) = D^{-a} g(w/D^b), \quad (2.5)$$

where  $g(x) \rightarrow x^{-c}$  as  $x \rightarrow 0$  [with a cutoff at  $w$  of  $O(1)$ ].

The normalization constraints,  $\int_0^\infty dw Q_D(w) = 1$  and  $\int_0^\infty dw w Q_D(w) = D$ , yield the conditions

$$a = bc, \quad 1 + a = 2b, \quad (2.6)$$

so that there is only one free exponent. For  $d=2$ , the random walk argument at the beginning of this section suggests that  $b = \frac{3}{2}$  [8] which agrees with the exact result [11]. For  $d > 2$ , random walks are less likely to coalesce, and this argument breaks down. In mean field theory one obtains the analytic result  $b=2$  [10], and exact analytic results for directed Abelian sandpiles in all dimensions [12] show that mean field theory is valid for  $d \geq 3$  (with logarithmic corrections in  $d=3$ ), and confirm the result  $b = \frac{3}{2}$  for  $d=2$ . (Our exponent  $b$  can be identified with  $\alpha+1$  of Ref. [12].)

As  $D \rightarrow \infty$ , the argument of the scaling function  $g$  in Eq. (2.5) is small for any finite  $w$ . Thus, in the  $q_{0,1}$  limit of our model, the distribution of weights,  $Q(w)$ , is independent of  $D$  as  $D \rightarrow \infty$ , and is of a power-law form, and hence is infinitely broad.

### C. $q$ model away from criticality

The rest of this paper concerns probability distributions of the  $q$ 's that do not have the property that  $q$  takes on only the values 1 and 0. We argue that all such distributions lead to force distributions that differ qualitatively from those described in the previous section. The  $q_{0,1}$  limit is the only one that yields a power-law force distribution; other distributions lead to a much faster, typically exponential, decay. In addition, for other  $q$  distributions, the distribution for the *normalized* weight  $v = w/D$ ,  $P_D(v)$  converges to a fixed distribution  $P(v)$  as  $D \rightarrow \infty$ . In contrast, in the  $q_{0,1}$  limit, the quantity  $Q_D(w)$  converges to a fixed function. In this section we present evidence for these assertions via both numerical simulations and mean field analysis.

#### 1. Numerical simulations

Our numerical investigations all indicate that that for all  $q$  distributions except for the  $q_{0,1}$  limit, the normalized force

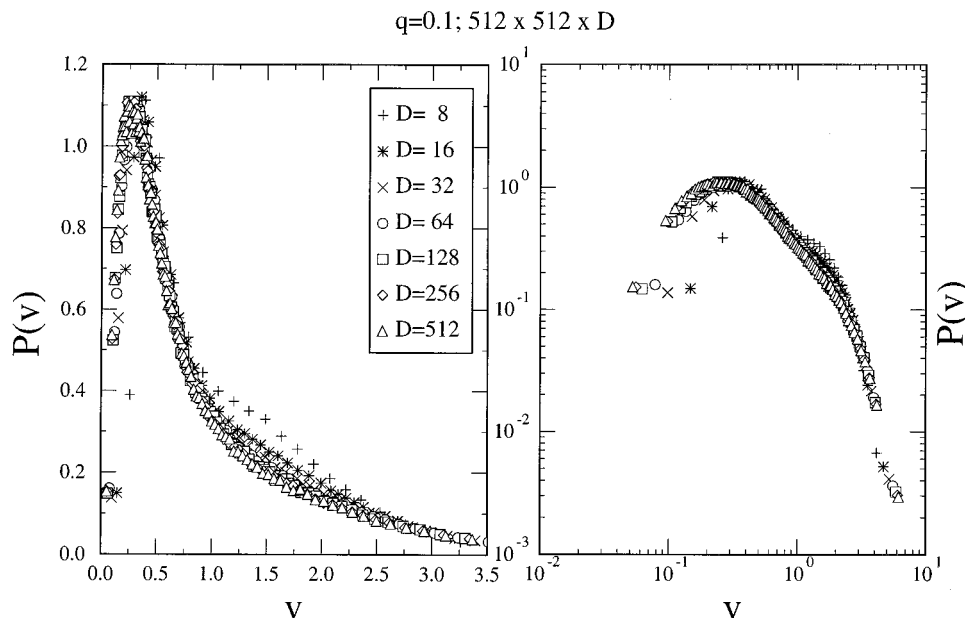


FIG. 2. Linear-linear and log-log plots of the normalized weight distribution function  $P_D(v)$  vs  $v$  for a three-dimensional system on fcc lattice ( $N=3$ ), for the  $q$  distribution defined in Eq. (2.7) with  $q_0=0.1$ . The distribution  $P_D(v)$  appears to become independent of  $D$  as  $D$  becomes large, and decays faster than a power law at large  $v$ .

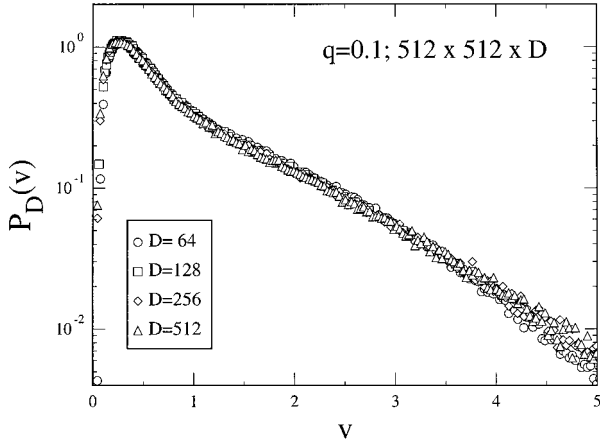


FIG. 3. Semilog plot of the normalized weight distribution function  $P_D(v)$  vs  $v$  for a three-dimensional system on a fcc lattice ( $N=3$ ), for the  $q$  distribution defined in Eq. (2.7) with  $q_0=0.1$ . The behavior of  $P_D(v)$  at large  $v$  is consistent with exponential decay.

distribution  $P_D(v)$  becomes independent of  $D$  as  $D \rightarrow \infty$ . To illustrate typical behavior, we consider the specific  $q$  distribution consisting of  $N-1$  bonds emanating down from each site with value  $q=q_0 < 1/(N-1)$  and one bond with  $q=1-(N-1)q_0$ , which has the induced distribution

$$\eta_{q_0}(q) = \frac{1}{N} \delta(q - [1 - \{N-1\}q_0]) + \frac{N-1}{N} \delta(q - q_0). \quad (2.7)$$

Figure 2 displays the normalized force distribution  $P_D(v)$  versus  $v$  for several different depths  $D$  in a three-dimensional fcc system ( $N=3$ ) of dimension  $512 \times 512 \times D$ , with  $q_0=0.1$ . Periodic boundary conditions are imposed in the transverse directions. As  $D$  becomes large,  $P_D(v)$  converges to a function independent of  $D$  which decays faster than a power law. Figure 3 is a semilog plot of  $P_D(v)$  versus  $v$  for several values of  $D$ , showing that the decay of  $P(v)$  at large  $D$  is roughly exponential. To see that this behavior is qualitatively different from that of the  $q_{0,1}$  limit, in Fig. 4 we

display numerical results for  $P_D(v)$  versus  $v$  for a system which is identical except that  $q_0=0$ . In contrast to the  $q=0.1$  case,  $P_D(v)$  decays as a power law at large  $v$ . Also,  $P_D(v)$  shows no signs of becoming independent of  $D$  as  $D \rightarrow \infty$ . This is consistent with the result in the previous section that  $Q_D(w)$  becomes independent of  $D$  at large  $D$ .

2. Mean field theory

The technique of the mean field analysis for a general  $q$  distribution is a generalization of that used for the  $q_{0,1}$  case [10]. The weight supported by a given site at depth  $D$ ,  $w_i(D)$ , depends not only on the weight supported by the sites at depth  $D-1$  but on the values of  $q$  for the relevant bonds:

$$w_i(D) = \sum_j q_{ij} w_j(D-1) + 1. \quad (2.8)$$

In general the values of  $w$  at neighboring sites in layer  $D$  are not independent; the mean field approximation consists of ignoring these correlations.

As discussed above, when  $q$  is allowed to take on values other than 0 and 1, it is useful to study the force distribution function as a function of the normalized weight at a given depth,  $v=w/D$ . In terms of the normalized weight variable  $v$ , the mean field approximation leads to a recursive equation for the weight distribution function  $P_D(v)$ :

$$P_D(v) = \prod_{j=1}^N \left\{ \int_0^1 dq_j \eta(q_j) \int_0^\infty dv_j P_{D-1}(v_j) \right\} \times \delta \left( \sum_{j=1}^N [(D-1)/D] v_j q_j - (v-1/D) \right). \quad (2.9)$$

The quantity  $\eta(q)$  is defined in Eq. (2.2). The constraint that the  $q$ 's emanating downward from a site must sum to unity enters only through the definition of  $\eta(q)$  because there is no restriction on the  $q$ 's for the ancestors of a site. The only approximation here is the neglect of possible correlations between the values of  $v$  among the ancestors.

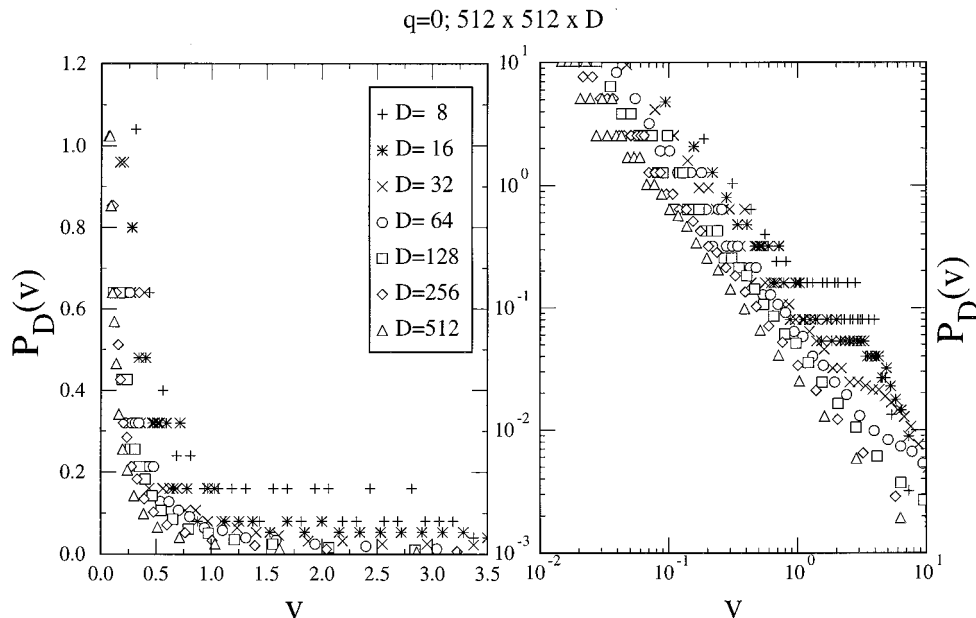


FIG. 4. Linear-linear and log-log plots of the normalized weight distribution function  $P_D(v)$  vs  $v$  for a three-dimensional system on a fcc lattice ( $N=3$ ), for the  $q$  distribution defined in Eq. (2.7) with  $q_0=0$ . For this special case, the distribution  $P_D(v)$  does not become independent of  $D$  as  $D$  becomes large. The asymptotic decay of  $P_D(v)$  at large  $v$  is a power law.

By Laplace transforming, one finds that  $\tilde{P}_D(s)$ , the Laplace transform of the distribution function of the normalized weight  $P_D(v)$ , obeys

$$\tilde{P}_D(s) = e^{-s/D} \left[ \int_0^1 dq \eta(q) \tilde{P}_{D-1}[sq(D-1)/D] \right]^N. \quad (2.10)$$

Since as  $D \rightarrow \infty$  the distribution  $P_D(v)$  becomes independent of  $D$  [17,18], Eq. (2.10) then becomes

$$\tilde{P}(s) = \left[ \int_0^1 dq \eta(q) \tilde{P}(sq) \right]^N. \quad (2.11)$$

First we show that the weight distribution  $P(v)$  decays faster than any power of  $v$  for all  $q$  distributions except those that only take on the values 0,1. We expand the Laplace transform  $\tilde{P}(s)$  in powers of  $s$ ,  $\tilde{P}(s) = 1 + \sum_{j=1}^{\infty} P_j s^j$ , and plug into Eq. (2.11), obtaining

$$1 + P_1 s + \sum_{j=2}^{\infty} P_j s^j = \left[ 1 + P_1 s/N + \sum_{j=2}^{\infty} P_j s^j \langle q^j \rangle \right]^N. \quad (2.12)$$

Here,  $s$  is the Laplace transform variable,  $\langle q^j \rangle = \int_0^1 dq q^j \eta(q)$ , and we have used  $\langle q \rangle = 1/N$ . Equating the coefficients of  $s^j$  on the left and right hand sides of the equation, we obtain a linear equation for  $P_j$ :

$$P_j [N \langle q^j \rangle - 1] = G(P_{j-1}, P_{j-2}, \dots, P_1), \quad (2.13)$$

where  $G$  is some complicated polynomial. This can be iterated to obtain  $P_j$  for successively higher values of  $j$ .

Since Eq. (2.13) is linear in  $P_j$ ,  $P_j$  can diverge only if its coefficient  $[N \langle q^j \rangle - 1]$  is zero. If  $q$  can take on only the values 0 and 1, then  $\langle q^j \rangle = \langle q \rangle$  and  $[N \langle q^j \rangle - 1] = 0$  for all  $j > 1$ . However, for *any* other distribution of  $q$ 's restricted to the interval  $[0, 1]$ , the distribution for  $q^j$  is shifted towards the origin compared to the distribution for  $q^k$ , whenever  $j > k$ . Since  $\langle q^j \rangle < \langle q \rangle = 1/N$  for all  $j > 2$ , Eq. (2.13) has a nonzero coefficient for  $P_j$  for all  $j > 2$ , which means that all moments  $\langle v^j \rangle$  of  $P(v)$  are finite. (For the special case of  $j=1$ , the equation is degenerate;  $P_1$  is set by the normalization of  $v$ .) If  $\ln P(v)$  were to behave asymptotically as  $-a \ln v$ , then  $\langle v^j \rangle$  would diverge for all  $j > a-1$ . Hence  $P(v)$  must fall off faster than any power of  $v$  and  $(d \ln P(v)/d \ln v) \rightarrow -\infty$  as  $v \rightarrow \infty$ .

#### D. Weight distributions away from criticality: Mean field results

Now we consider the distribution of weights for noncritical distributions of  $q$ 's. Motivated by the geometrical disorder present in granular materials, we focus especially on continuous distributions. First we calculate this distribution within a mean field approximation for the simplest possible continuous distribution,  $f(q_{ij}) = \text{const}$ , or  $\rho(q_{i1}, \dots, q_{iN}) = (N-1)! \delta(\sum_j q_{ij} - 1)$  (the uniform  $q$  distribution). We show that within mean field theory, all "typical" continuous  $q$  distributions lead to a force distribution that decays exponentially at large weights. We will show later that the mean field solution is *exact* for a countable set of  $q$  distributions, including the uniform  $q$  distribution.

#### 1. Mean field theory for the uniform distribution

One example of a  $q$  distribution that can lead to an exponentially decaying distribution of weights is the "uniform" distribution of  $q$ 's, for which the probability of obtaining the values  $q_{i1}, \dots, q_{iN}$  is  $\rho(q_{i1}, \dots, q_{iN}) = (N-1)! \delta(\sum_j q_{ij} - 1)$ . We show in the Appendix that this distribution induces  $\eta_u(q) = (N-1)(1-q)^{N-2}$ . Thus, for this  $q$  distribution in the limit  $D \rightarrow \infty$  the mean field force distribution is the solution to the self-consistent equation:

$$\tilde{P}(s) = \left[ \int_0^1 dq (N-1)(1-q)^{N-2} \tilde{P}(sq) \right]^N. \quad (2.14)$$

First consider  $N=2$ . For this case  $\eta(q) = 1$ , so Eq. (2.14) becomes

$$\tilde{P}(s) = \left[ \int_0^1 dq \tilde{P}(sq) \right]^2. \quad (2.15)$$

Letting  $\tilde{V}(s) = [\tilde{P}(s)]^{1/2}$  and  $u = qs$ , one obtains

$$s \tilde{V}(s) = \int_0^s du \tilde{V}^2(u). \quad (2.16)$$

Differentiating with respect to  $s$  yields

$$\tilde{V}(s) + s \frac{d\tilde{V}}{ds} = \tilde{V}^2(s), \quad (2.17)$$

which can be integrated to yield

$$\tilde{V}(s) = \frac{1}{1-Cs}. \quad (2.18)$$

The constant of integration  $C$  is determined by the definition of the mean,  $\int_0^\infty dv v P(v) = -d\tilde{P}/ds|_{s=0} = 1$ . Thus,  $C = d\tilde{V}/ds|_{s=0} = -\frac{1}{2}$ . Hence one finds  $\tilde{P}(s) = 4/(s+2)^2$  and  $P(v) = 4v e^{-2v}$ .

This method can be generalized for all  $N$ . Defining  $\tilde{V}_N(s) = [\tilde{P}_N(s)]^{1/N}$ , inserting in Eq. (2.14), and differentiating  $N-1$  times, one finds that  $\tilde{V}_N(s)$  obeys the differential equation:

$$\frac{d^{N-1}}{ds^{N-1}} [s^{N-1} \tilde{V}_N(s)] = (N-1)! \tilde{V}_N^N(s). \quad (2.19)$$

A solution to this equation is  $\tilde{V}_N(s) = C/(s+C)$ , where  $C$  is any constant. This can be shown by induction: Assume that

$$\frac{d^{N-2}}{ds^{N-2}} \left( s^{N-2} \frac{C}{s+C} \right) = (N-2)! \left( \frac{C}{s+C} \right)^{N-1}. \quad (2.20)$$

Then

$$\frac{d^{N-1}}{ds^{N-1}} \left( s^{N-1} \frac{C}{s+C} \right) = \frac{d^{N-1}}{ds^{N-1}} \left( (s+C-C)s^{N-2} \frac{C}{s+C} \right) \tag{2.21}$$

$$= -C \frac{d}{ds} \left[ (N-2)! \left( \frac{C}{s+C} \right)^{N-1} \right] \tag{2.22}$$

$$= (N-1)! \left( \frac{C}{s+C} \right)^N. \tag{2.23}$$

Since direct substitution can be used to show that the identity holds for  $N=2$ , it holds for all  $N$ .

The condition  $d\tilde{V}/ds = -1/N$  is satisfied when  $C=N$ . Hence one finds the weight distribution:

$$P_N(v) = \frac{N^N}{(N-1)!} v^{N-1} e^{-Nv}. \tag{2.24}$$

The question of uniqueness of this solution is discussed below.

**2. Mean field asymptotic force distribution for generic continuous  $q$  distributions**

We now show that, within mean field theory, generic continuous  $q$  distributions lead to weight distribution functions  $P(v)$  for the normalized weight  $v$  which have the asymptotic forms  $P(v) \propto v^{N-1} e^{-Nv}$  as  $v \rightarrow \infty$  and  $P(v) \propto v^{N-1}$  as  $v \rightarrow 0$ .

We consider  $q$  distributions of the form  $\rho(q_{i1}, \dots, q_{iN}) = \{ \prod_j f(q_{ij}) \} \delta(\sum_j q_{ij} - 1)$  [the uniform distribution is  $f(q_{ij}) = \text{const}$ ]. If  $f(q_{ij})$  has a nonzero limit as  $q_{ij} \rightarrow 0$ , and does not have a  $\delta$ -function contribution at  $q_{ij} = 0$ , then phase space restrictions imply that the induced distribution  $\eta(q) \sim (1-q)^{N-2}$  for  $q \rightarrow 1$ . This is because if a site receives a fraction  $q$  of the weight from one of its predecessors, then the fractions received by all the *other* successors of that predecessor,  $\{q_2 \dots q_N\}$ , must add up to  $1-q$ . For  $q$  close to 1, this gives a phase-space volume of the order of  $(1-q)^{N-2}$ .

To determine the large  $v$  asymptotics of  $P(v)$ , we use the result of Sec. II C 2, that  $P(v)$  must fall off faster than any power of  $v$ . We write the  $D \rightarrow \infty$  limit of Eq. (2.9) as

$$P(v) = \left\{ \prod_{j=1}^N \int_0^\infty dv_j F(v_j) \right\} \delta \left( v - \sum_j v_j \right), \tag{2.25}$$

$$F(v_j) = \int_0^1 dq_j P(v_j/q_j) \eta(q_j)/q_j. \tag{2.26}$$

Since  $P(v)$  decays quickly (in particular, faster than  $1/v$ ), the apparent singularity near  $q=0$  in Eq. (2.26) is not really there. The integral is dominated by  $q \approx 1$ . This follows because

$$\begin{aligned} P(v/q) &= P(v) \exp \left[ - \left. \frac{\partial \ln P(v/q)}{\partial q} \right|_{q=1} (1-q) + \dots \right] \\ &= P(v) \exp \left[ \frac{v}{q^2} \left. \frac{\partial \ln P(v/q)}{\partial (v/q)} \right|_{q=1} (1-q) + \dots \right] \\ &= P(v) \exp \left[ \left. \frac{\partial \ln P(u)}{\partial \ln u} \right|_{u=v} (1-q) + \dots \right]. \end{aligned} \tag{2.27}$$

Since  $\partial \ln P(u)/\partial \ln u \rightarrow -\infty$  as  $u \rightarrow \infty$ , this expression becomes very small as  $1-q$  increases. Thus, for large  $v$ , since  $\eta(q) \sim (1-q)^{N-2}$  for  $q \approx 1$ ,

$$F(v) \sim P(v) \left/ \left[ \left| \frac{\partial \ln P(v)}{\partial \ln v} \right| \right]^{N-1} \right. . \tag{2.28}$$

Already it is clear that  $P(v)$  for any generic  $q$  distribution has the same large- $v$  asymptotics as the uniform distribution, since the asymptotics are determined entirely by the phase-space restrictions on  $\eta(q)$  for  $q \approx 1$ . This decay also can be demonstrated explicitly by assuming faster and slower decays and showing inconsistency with Eq. (2.25). If  $P(v)$  were to decay faster than exponentially, then the convolution in Eq. (2.25) would be dominated by the region where all the  $v_j$ 's are roughly equal. But since  $[P(v/N)]^N \gg P(v)$ , Eq. (2.25) cannot be satisfied. On the other hand, if  $P(v)$  were to decay slower than exponentially, then the convolution would be dominated by the region where one of the  $v_i$ 's is  $\approx v$  and the others are  $O(1)$ . Equation (2.25) would then imply

$$P(v) \sim P(v) \left/ \left[ \left| \frac{\partial \ln P(v)}{\partial \ln v} \right| \right]^{N-1} \right. . \tag{2.29}$$

Since the expression in square brackets diverges with  $v$ , this is not possible either. Thus one must have  $P(v) = h(v) \exp[-av]$ , where  $h(v)$  varies more slowly than an exponential. Equation (2.25) then implies

$$h(v) = \left\{ \prod_{j=1}^N \int_0^\infty dv_j h(v_j)/v^{N-1} \right\} \delta \left( v - \sum_j v_j \right). \tag{2.30}$$

This is satisfied by  $h(v) \sim v^{N-1}$ , so that

$$P(v) \sim v^{N-1} \exp[-av] \tag{2.31}$$

for  $v \rightarrow \infty$ .

Hence we have shown that for generic continuous  $q$  distributions, within mean field theory  $P(v) \rightarrow v^{N-1} \exp(-av)$  as  $v \rightarrow \infty$ .

**3. Mean field theory for singular  $q$  distributions**

We have shown that all  $q$  distributions which satisfy the condition  $\int_0^1 dq \eta(q) \sim (1-q)^{N-1}$  as  $q \rightarrow 1$  have a weight distribution within mean field theory that is of the form  $P(v) \sim v^{N-1} \exp[-av]$  for large  $v$ . This condition on  $\eta(q)$  is satisfied under fairly general assumptions: one requires (1) that the probability density for any  $q_{ij}$  in Eq. (2.8) have a nonzero  $q_{ij} \rightarrow 0$  limit and (2) that it not have a  $\delta$ -function

contribution at  $q_{ij}=0$ . However, as we shall see below, to compare the results of the  $q$  model to molecular dynamics simulations and to experiments on real bead packs, it is useful to consider the case where there is a finite probability for some of the  $q_{ij}$ 's to be zero, which implies that the induced distribution  $\eta(q)$  has a  $\delta$  function at  $q=0$  (and in some cases at  $q=1$ ) [19]. Such a choice for  $\eta(q)$  is also useful in examining the crossover from the critical  $q_{0,1}$  limit to the smooth  $q$  distributions considered in the preceding section. We will see that  $q$  distributions of this type lead to force distributions  $P(v)$  that decay exponentially, though with different power laws multiplying the exponential than for continuous  $q$  distributions.

We first note that, when  $\eta(q)$  has a finite weight at  $q=1$ , it is impossible for  $\tilde{P}(s)$  to diverge at any  $s$ . The solutions of the form  $\tilde{P}(s) \sim 1/(q+s/s_0)^N$  obtained in Sec. II D 1 were possible because, in Eq. (2.11), the integral over  $q$  reduces the singularity, which is compensated by the exponentiation. With a finite weight at  $q=1$ , close to a divergence at  $s_0$  one would have  $\tilde{P}(s) \propto [\tilde{P}(s)]^N$ , which would be impossible as  $s \rightarrow s_0$ .

It is instructive to consider first a simplified version of such singular  $q$  distributions. Let us consider the case of  $N=2$ , and assume that  $\eta(q)$  has the form

$$\eta(q) = \frac{1}{2}(1-\theta)\{\delta(q) + \delta(1-q)\} + \theta\delta(q - \frac{1}{2}), \quad (2.32)$$

with  $0 < \theta < 1$ . This  $\eta(q)$  satisfies the conditions  $\int dq \eta(q) = 1$  and  $\int dq q \eta(q) = \frac{1}{2}$  for all  $\theta$ . Equation (2.11) then simplifies to

$$\tilde{P}(s) = [\frac{1}{2}(1-\theta) + \frac{1}{2}(1-\theta)\tilde{P}(s) + \theta\tilde{P}(s/2)]^2, \quad (2.33)$$

where we have used the fact that  $\tilde{P}(0)=1$ . Equation (2.33) can be solved as follows: for small  $s$ , we know that  $\tilde{P}(s) = 1 - s + O(s^2)$  [the coefficient of the linear term being fixed by the normalization condition  $\int dv v P(v) = 1$ ]. Starting with a small negative value of  $s$ , where  $\tilde{P}(s)$  is approximated as  $1-s$ , Eq. (2.33) can be iterated to find  $\tilde{P}(2^n s)$  for  $n=1,2,\dots$  [the correct root of the quadratic equation is chosen by requiring  $\tilde{P}(s)=1$  for  $\tilde{P}(s/2)=1$ ]. Eventually the result of this iteration scheme is complex rather than real, signifying that  $s$  is in a region where  $\tilde{P}(s)$  has a branch cut. It is easiest to find the origin  $s_0$  of this branch cut by adjusting  $\tilde{P}(s_0/2)$  so that Eq. (2.33) has a double root for  $\tilde{P}(s_0)$ , and then iterating *backwards* to obtain  $\tilde{P}(s_0/2^n)$ . As  $n \rightarrow \infty$ , by matching on to the requirement that  $\tilde{P}(s) = 1 - s$  for  $s \rightarrow 0$ , one can obtain  $s_0$ . It is clear from Eq. (2.33) that in the vicinity of  $s_0$   $\tilde{P}(s)$  is of the form  $\tilde{P}(s_0) + \alpha\sqrt{s-s_0}$ . This yields

$$P(v) \sim v^{-3/2} \exp[-s_0 v] \quad \text{for } v \rightarrow \infty. \quad (2.34)$$

Although the power-law prefactor is different from that in Eq. (2.31), there is still an exponential decay.

We now consider possible changes to Eq. (2.34) from choosing  $\eta(q)$  of a more complicated form than Eq. (2.32). For any  $\eta(q)$  of the form

$$\eta(q) = \sum_{i=0}^n c_i \delta(q - \lambda^i) + \left(1 - \sum c_i\right) \delta(q) \delta(q) \quad (2.35)$$

with  $0 < \lambda < 1$ , one can use the method outlined above to find that  $\tilde{P}(s)$  has a square-root branch cut at some  $s_0$ . This answer is not affected by making  $n$  large, so long as  $c_0$  remains nonzero. As  $n \rightarrow \infty$ , with all the  $c_i$ 's for  $i > 0$  tending to zero, we can approach arbitrary continuous distributions for  $\eta(q)$  with  $\delta$  functions at  $q=0$  and  $q=1$ .

For  $N > 2$ , Eq. (2.33) is changed to a higher order equation. This, however, does not generically change the results above. Even for higher order equations, the degeneracy of the roots generally occurs only pairwise, so that close to the point of degeneracy the singularly ranging roots still have a square-root singularity. It will, however, be possible to find *nongeneric* choices for  $\eta(q)$  that could result in an asymptotic form  $P(v) \sim v^{-(1+1/m)} \exp[-av]$  with  $N \geq m \geq 2$ .

## E. Beyond mean field theory

### 1. Proof that mean field theory is exact

In this section we prove that the mean field solution presented in the preceding section is an *exact* solution of the model with the uniform  $q$  distribution for any  $N$ .

In general, the mean field theory presented above is not exact because it does not account for the fact that two neighboring sites in row  $D+1$  both derive a fraction of their weight from the same site in row  $D$ . Suppose a site  $j$  in row  $D+1$  has  $w(j)$  much larger than the average value. Then it is likely that the weight supported by an ancestor  $w(i)$  in row  $D$  is larger than average also. Because this ancestor transmits its weight to a neighboring site in row  $D+1$  as well, there is a ‘‘correlation’’ effect that creates a greater likelihood that in a given layer sites supporting large weight are close together. On the other hand, there is a ‘‘anticorrelation’’ effect arising because  $\sum_j q_{ij} = 1$ ; if a large fraction of the weight from site  $i$  is transmitted to site  $j$ , then small fractions are transmitted to the other ‘‘offspring’’ sites. When the  $q$ 's are chosen from the uniform distribution, these ‘‘correlation’’ and ‘‘anticorrelation’’ effects cancel exactly.

The result that the mean field correlation functions are exact for the uniform distribution of  $q$ 's can be understood by considering the system in terms of weights on bonds. Each bond  $\{ij\}$  corresponds to a particle with ‘‘energy’’  $E_{ij} = v_i q_{ij}$ . Moving down by one layer corresponds to having groups of  $N$  particles colliding at each site and emerging with different energies, subject to the constraint that the total energy of all  $N$  particles colliding at each site is unchanged by the collision.

For the ‘‘uniform’’  $q$  distribution, each collision takes  $N$  particles of energies  $e_{\alpha_1}, \dots, e_{\alpha_N}$  and changes their energies to  $E_{\alpha_1}, \dots, E_{\alpha_N}$ , subject only to the constraint that  $\sum e_{\alpha} = \sum E_{\alpha}$ . If we start with a ‘‘microcanonical’’ ansatz for the phase-space density, i.e., that it is uniform over the space  $\sum E_{\alpha} = E$ , then it is preserved by the collisions. Hence, the microcanonical density is the correct one for this system.

With a microcanonical density for a large collection of particles, the density for any finite subgroup is canonical (in the thermodynamic limit) [20]. Thus, we have shown for this case that the distribution of ‘‘bond forces’’ is exponential, which is the most random distribution consistent with the constraint that the sum of the forces is fixed [20,21].

Note that this argument does not hold for  $q$  distributions other than the uniform one. For instance, in the  $q_{0,1}$  limit,

each collision takes all the energy of the group and gives it to one of the colliding particles. Thus, even if we start with the microcanonical distribution, it breaks down at the very first step. For general  $q$  distributions, the phase-space density is not separable, i.e., mean field theory is not exact and there are spatial correlations within each layer.

The explicit algebraic proof proceeds by constructing exact recursion relations for the correlation functions describing the weight distribution in the model in row  $D+1$  in terms those for row  $D$ , and showing that the mean field correlation functions are invariant under this recursion. We ignore the weight added in each row because we are looking for the fixed distribution very far down the pile.

Let  $P_D(u_i)$  be the probability that site  $i$  in row  $D$  supports weight  $u_i$ ,  $P_D(u_{i_1}, u_{i_2})$  be the probability that sites  $i_1$  and  $i_2$  support weight  $u_{i_1}$  and  $u_{i_2}$ , respectively, and  $P_D(u_{i_1}, u_{i_2}, \dots, u_{i_n})$  be the normalized joint distribution describing the probability that sites  $i_1, i_2, \dots, i_n$  support weights  $u_{i_1}, \dots, u_{i_n}$ , respectively. The mean field joint probability distributions are given by the mean field  $P(u)$  and

$$P(u_1, u_2, \dots, u_n) = P(u_1)P(u_2) \cdots P(u_n). \quad (2.36)$$

Consider the  $M$ -point correlation function in row  $D+1$  that is obtained when all the correlation functions in row  $D$  are the the mean field ones. Let  $\{u_i\}$  be the weights in row  $D$  and  $\{v_j\}$  be the weights in row  $D+1$ . Consider a cluster of sites  $j=1, \dots, M$  in row  $D+1$ , with ancestors in row  $D$  at sites  $i=1, \dots, p$ . (The labels do not imply any particular spatial relation of the sites.) The  $q$ 's describing the bonds emanating from ancestor  $i$  are  $q_{il}$ , where  $l=1, \dots, N$ . We define  $\eta_{il}(j)$  to be 1 if sites  $i$  and  $j$  are connected by bond  $il$  and zero otherwise. The  $M$ -point correlation function in row  $D+1$ ,  $P_{D+1}(v_1, \dots, v_M)$ , must obey

$$\begin{aligned} P_{D+1}(v_1, \dots, v_M) &= \prod_{i=1}^p \left\{ \int_0^1 dq_{i1} \cdots \int_0^1 dq_{iN} (N-1)! \right. \\ &\quad \times \delta \left( 1 - \sum_{k=1}^N q_{ik} \right) \int_0^\infty du_i P_D(u_i) \left. \right\} \\ &\quad \times \prod_{j=1}^M \delta \left( v_j - \sum_{i=1}^p \sum_{l=1}^N \eta_{il}(j) q_{il} u_i \right). \end{aligned} \quad (2.37)$$

We define the general Laplace transform

$$\begin{aligned} \tilde{P}(s_1, \dots, s_n) &= \int_0^\infty dv_1 \cdots \int_0^\infty dv_n P(v_1, \dots, v_n) \\ &\quad \times e^{-s_1 v_1 - \cdots - s_n v_n}. \end{aligned} \quad (2.38)$$

Laplace transforming Eq. (2.37), one obtains

$$\begin{aligned} \tilde{P}_{D+1}(s_1, \dots, s_M) &= \prod_{i=1}^p \int_0^1 dq_{i1} \cdots \int_0^1 dq_{iN} (N-1)! \\ &\quad \times \delta \left( 1 - \sum_{k=1}^N q_{ik} \right) \\ &\quad \times \tilde{P}_D \left( \sum_{j=1}^M \sum_{l=1}^N \eta_{il}(j) q_{il} s_j \right). \end{aligned} \quad (2.39)$$

For  $\tilde{P}_D(x) = (1+x/N)^{-N}$ , one can use the condition  $\sum_{l=1}^N q_{il} = 1$  to write

$$\begin{aligned} \tilde{P}_{D+1}(s_1, \dots, s_M) &= \prod_{i=1}^p \int_0^1 dq_{i1} \cdots \int_0^1 dq_{iN} (N-1)! \\ &\quad \times \delta \left( 1 - \sum_{k=1}^N q_{ik} \right) \\ &\quad \times \left[ \sum_{l=1}^N q_{il} \left( 1 + \sum_{j=1}^M \eta_{il}(j) s_j / N \right) \right]^{-N}. \end{aligned} \quad (2.40)$$

Using the identity [22]

$$\begin{aligned} \prod_{n=1}^N (a_n)^{-1} &= (N-1)! \\ &\quad \times \int_0^1 dx_1 \cdots \int_0^1 dx_N \frac{\delta(1-x_1-\cdots-x_N)}{(a_1 x_1 + \cdots + a_N x_N)^N} \end{aligned} \quad (2.41)$$

with  $a_n = 1 + \sum_{j=1}^M \eta_{in}(j) s_j / N$ , one finds

$$\tilde{P}_{D+1}(s_1, \dots, s_M) = \prod_{i=1}^p \prod_{n=1}^N \frac{1}{1 + \sum_{j=1}^M \eta_{in}(j) s_j / N}. \quad (2.42)$$

If a given bond  $\{in\}$  connects to no sites in the descendant cluster, then every term in the sum in the denominator of Eq. (2.42) is zero, and the  $\{in\}$ th term in the product is unity. If the bond connects to a site in the descendant cluster, then  $\eta_{in}(j)$  is unity for exactly one  $j$ . Each site  $j$  in the descendant cluster is connected to exactly  $N$  antecedents in row  $D$ , so

$$\tilde{P}_{D+1}(s_1, \dots, s_M) = \prod_{j=1}^M \frac{1}{(1 + s_j / N)^N}. \quad (2.43)$$

Thus, the mean field correlation functions are preserved from row to row for this  $q$  distribution.

### 2. Other $q$ distributions

We have identified a countable set of  $q$  distributions for which mean field theory is exact, those of the form  $f(q_{ij}) = q^r$ , for all integer  $r$  (the uniform distribution is  $r=0$ ). The resulting force distribution  $P_r(v) \propto v^{r+N-1} e^{-Nr v}$  has Laplace transform  $\tilde{P}_r(s) = [1 + s/(Nr)]^{-Nr}$ . The demon-

stration that this solution is exact follows precisely the same line of reasoning as for the  $r=0$  case presented in the preceding section, utilizing the identity [22]

$$\prod_{n=1}^N (a_n)^{-r} = \frac{\Gamma(Nr)}{[\Gamma(r)]^N} \int_0^1 dx_1 x_1^{r-1} \cdots \int_0^1 dx_N x_N^{r-1} \times \frac{\delta(1-x_1-\cdots-x_N)}{(a_1 x_1 + \cdots + a_N x_N)^{Nr}}. \quad (2.44)$$

In terms of the particle collision picture discussed at the beginning of Sec. II E 1, a general value of  $r$  corresponds to the particles having an energy which is the sum of  $r+1$  components (which may be viewed as spatial coordinates in some underlying space), each one of which is conserved individually in a collision. The microcanonical phase-space density, uniform in the  $N(r+1)$ -dimensional space, is preserved by the collisions, and yields the  $P_r(v)$  stated here.

The result that mean field theory yields an exact solution of the model holds only for a very limited class of  $q$  distributions. For general  $q$  distributions, the phase-space density is not separable, i.e., mean field theory is not exact, and there are spatial correlations within each layer. For example, Fig. 5 shows  $P(v)$  for a two-dimensional system with  $N=2$  and the  $q$  distribution where the two bonds emanating from each take on the values  $q_0$  and  $1-q_0$ , with  $q_0=0.1$ . In the model, a site  $(i,D)$  is connected to sites  $(i,D+1)$  and  $[(i+1) \bmod L, D+1]$ ; in the mean field calculation, site  $(i,d)$  is connected to sites  $(p_1(i), D+1)$  and  $(p_2(i), D+1)$ , where  $p_1$  and  $p_2$  are permutations of  $(1, \dots, L)$ . This method of simulating mean field theory destroys the spatial correlations between ancestor sites, while ensuring that every site has exactly two ancestors and two descendants. The numerical data were obtained by averaging  $P(v)$  for rows 10 001–20 000 in a system of transverse extent  $L=20\,000$ . This figure demonstrates explicitly that the mean field force distribution  $P(v)$  is not exact for this distribution. However, the deviations of the mean field theory from the direct simulation are ex-

remely small for  $v \geq 0.1$ , so mean field theory provides an accurate quantitative estimate for  $P(v)$  over a large range of  $v$ .

### 3. Uniqueness of the steady state distribution

In this section we show that our results (numerical and analytical) for the force distribution do not depend on either the boundary conditions imposed at the top of the system or on the specific realization of randomness a particular system might have.

Consider a system of finite transverse extent  $L$ , in which weights  $\{w(i)\}$  are put on the particles in the top row. The weight then propagates downwards according to Eq. (2.8). If we now consider the same system with a different loading on the top row,  $\{w(i) + \delta w(i)\}$ , then since Eq. (2.8) is linear in  $w$ , the difference between the two solutions satisfies the homogeneous equation

$$\delta w(D+1, j) = \sum_i q_{i,j}(D) \delta w(D, i). \quad (2.45)$$

Summing up both sides, we see that  $\sum_j \delta w(D+1, j) = \sum_i \delta w(D, i)$ , which means that the total excess weight placed on the top of the system propagates downwards unaltered. Such a change only affects the normalization of our distributions. Thus, if we are interested in the normalized distribution  $P_D(v)$ , we can without loss of generality consider perturbations  $\{\delta w(D, i)\}$  satisfying the constraint  $\sum_i \delta w(D, i) = 0$ .

Equation (2.45) can be viewed as a two stage process: (1) each  $\delta w(D, i)$  splits into  $N$  parts,  $q_{i,j}(D) \delta w(D, i)$ , and (2) the  $N$  fragments  $q_{i,j}(D) \delta w(D, i)$ , with  $i$  running over the neighbors of  $j$  in the row above it, combine to give  $\delta w(D+1, j)$ . The important thing is that all the  $q_{i,j}$ 's are positive. Thus if we define the total difference between the two configurations as  $\Delta(D) = \sum_i |\delta w(D, i)|$ , then because all the  $q$ 's are positive and  $\sum_j q_{ij} = 1$ ,  $\Delta$  is unchanged in the first step, while in the second step it can either stay constant or decrease (depending on whether the signs of the fragments are

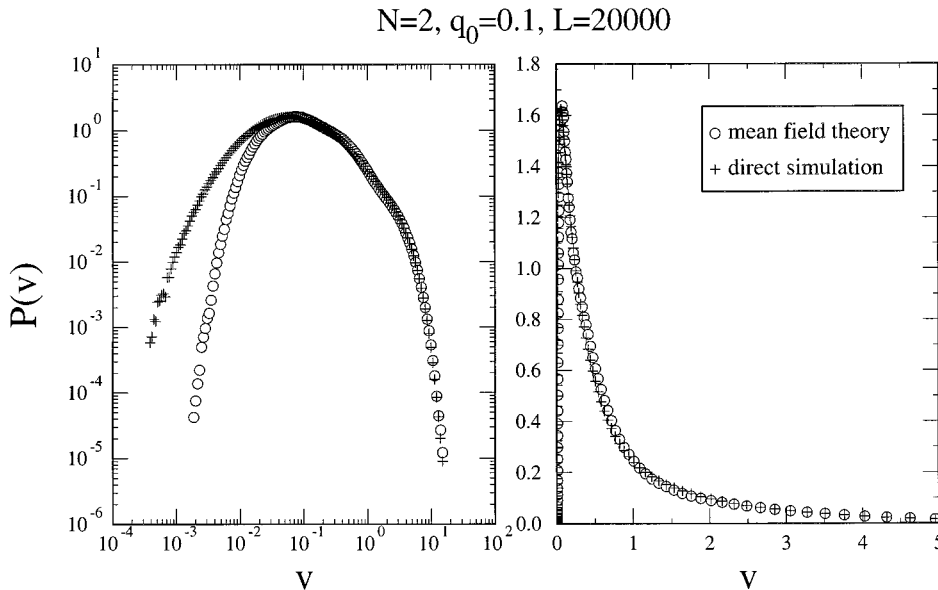


FIG. 5. Comparison of force distribution  $P(v)$  versus  $v$  for simulation of mean field theory and of the original model equations (2.1) for a system with the  $q$  distribution Eq. (2.7) with  $N=2$  and  $q_0=0.1$ . Both data sets were obtained by averaging the bottom 10 000 rows of a 20 000  $\times$  20 000 system. Mean field theory does not yield the exact  $P(v)$  for this  $q$  distribution. Nonetheless, it provides an accurate quantitative estimate for  $P(v)$  over a broad range of  $v$ .

the same or different). Further, while for any *particular* value of  $D$  it is possible for  $\Delta(D)$  to be equal to  $\Delta(D+1)$ , the only way in which  $\Delta(D)$  can remain unchanged as  $D$  increases is if all the positive  $\delta w$ 's are segregated from all the negative ones. Even if this is the case in the top row, this becomes increasingly unlikely as  $D$  is increased. In fact, if the minimum distance between positive and negative  $\delta w$  is  $l$  in the top row, and if there are no  $\delta$  functions in  $\eta(q)$ , then  $\Delta(D+1)$  *must* be less than  $\Delta(D)$  for  $D>l$ . Thus for a system of finite transverse extent, the distribution of weights at the bottom of the system is independent of the loading on the top row in the limit that the height of the system is infinite. For the case when all dimensions of the system are made infinite the situation is trickier; due to the conservation of  $\Sigma \delta w$  under the evolution of Eq. (2.45) discussed above, if one were to make  $\delta w$  positive on one side of the top row and negative on the other half, for a system of transverse extent  $L$  it would require a height  $O(L^2)$  for the effects of this perturbation to ‘‘diffuse’’ away. For generic loading at the top, however, we do not expect such an anomalous concentration of fluctuations into only the longest wavelength modes of the system, and  $\Delta(D)$  should decay with  $D$  even if all dimensions of the system are enlarged.

We have seen that the distribution of weight at the bottom of any infinite system is independent of the details of how forces are distributed at the top, at least in the limit when the height of the system is taken to infinity before its transverse dimensions. This is true for each system individually, and is therefore also true for the full ensemble of systems with different realizations of randomness (the choice of  $q_{ij}$ 's), so that the solutions we have obtained so far for quantities like  $P(v)$  are unique. For any particular system, however, the weights on the different sites at the bottom *do* depend on the  $q_{ij}$ 's; in fact, with all the  $q_{ij}$ 's specified, the weights on the different sites are completely determined. Even for a single system, however, statistics can be obtained by measuring quantities across all the sites in the bottom row; for a system of infinite transverse size the measurements then lead to distributions. At least for the ‘‘uniform’’  $q$  distribution, any quantity like, say,  $P(v)$ , is the same, whether obtained by averaging over sites in a single system or for a single site over the entire ensemble. This is because, as we have seen, the ensemble averaged distribution of  $\{v_1, \dots, v_L\}$  across the bottom row is of the form  $P(v_1, \dots, v_L) = P(v_1)P(v_2) \cdots P(v_L)$ . For any single system chosen randomly from the ensemble, this is the probability density that the normalized weights in the bottom row take on the specific values  $\{v_1, v_2, \dots, v_L\}$ . The probability that  $l$  of these  $L$  sites will have  $v_i$  greater than some  $v_0$  is then

$$\binom{L}{l} \left( \int_{v_0}^{\infty} P(v) dv \right)^l \left( 1 - \int_{v_0}^{\infty} P(v) dv \right)^{L-l}; \quad (2.46)$$

as  $L \rightarrow \infty$ ,  $l/L$  is sharply peaked around  $\int_{v_0}^{\infty} P(v) dv$ , so that the site averaged result is the same as the ensemble average. We expect this to be the case even for more general  $q$  distributions, for which the ensemble averaged  $P(v_1, v_2, \dots, v_L)$  does not have a product form, so long as the transverse correlation lengths are finite.

### III. NUMERICAL SIMULATIONS OF SPHERE PACKINGS

We now discuss the relevance of the  $q$  model to granular materials. Although we have shown that the  $q$  model yields an exponentially decaying force distribution independent of the details of the  $q$  distribution, to make quantitative comparison of this model to granular systems, we must know the  $q$  distribution for a granular material. To make this comparison, we have performed molecular dynamics simulations of three-dimensional sphere packings, analyzed the contact distributions to estimate the distribution of  $q$ 's, and then calculated the force distribution in the sphere packing and compared it to that predicted by the  $q$  model. Our simulations yield results for the contact force distributions that are consistent with previous work [23–26]; the new ingredient here is that the geometry of the packing is characterized simultaneously, allowing testing of the statistical assumptions underlying the  $q$  model.

Our simulation consists of 500 spherical beads of weight and diameter unity in a uniform gravitational field with gravitational constant  $g=1$ , interacting via a central force  $F$  of the Hertzian form,  $F=F_0(\delta r)^{3/2}$ . Here,  $F_0$  is the force constant, chosen so that a sphere has a deformation of  $\delta r=0.001$  when subjected to its own weight, and  $\delta r$  is the deformation of each bead at the contact. The box containing the beads had a fixed bottom, and lateral dimensions of  $5.5 \times 5.5$ . In each simulation, the spheres are initially placed in a loose rectangular lattice with lattice constants of  $1 \times 1 \times 1.5$  and have random initial velocities uniformly distributed in the range  $-V_{\max} < V_{x,y,z} < V_{\max}$ , where  $V_{\max}=50$  is large enough to yield significantly different packings from run to run. By freezing the motion of the beads whenever the total kinetic energy of the system reaches a maximum, the kinetic energy of the system is reduced and eventually the spheres all settle to the bottom of the box. Starting with a flat bottom, the regularity of layerlike packing reduces as the height increases. A rough bottom was obtained by selecting the beads with height between  $H$  and  $H+1$  (typically,  $H \sim 10$ ) and this rough bottom was used for the next simulation. Within a few iterations, the statistical properties of the rough bottom becomes independent of its initial configuration; this configuration of spheres at the bottom of the box is then fixed and used as a boundary condition for subsequent packing simulations.

In our packings, a sphere can have up to six contacts on its bottom half. However, on average, the three strongest vertical forces at these contacts sustain over 98% of the load; three or fewer particles supported at least 90% of the weight for over 92% of the particles. Therefore, comparison with the  $q$  model with  $N=3$  is reasonable.

We estimate the  $q$  distribution for the sphere simulation by calculating the fractions of the total vertical force supported by each of the three strongest contacts [27]. To display our results for the  $q$  distribution for the simulation of hard spheres, we define the variables  $\alpha_1=(q_3-q_2)/\sqrt{3}$ ,  $\alpha_2=q_1$  [28]. Because  $\sum_{j=1}^3 q_j=1$ , the possible values of the  $\alpha$ 's can all be represented as points in the interior of an equilateral triangle, where the values of  $q$  are the perpendicular distances to each side of the triangle. Moreover, for the uniform  $q$  distribution, the density of points in the triangle is constant. If one orders the  $q$ 's so that  $q_3 > q_2 > q_1$ ,

then in terms of the  $\alpha$  variables, all the points lie in the triangle shown in Fig. 6, which is bounded by the lines  $\alpha_1 > 0$ ,  $\alpha_2 > 0$ , and  $\sqrt{3}\alpha_1 + \alpha_2 < 1$ . As Fig. 6 demonstrates, there is some deviation from the uniform  $q$  distribution because a nonzero fraction of the particles have  $q_1 = \alpha_2 = 0$ . A reasonable description of the numerically observed particle contact distribution is obtained by taking each particle and assigning with probability  $p$ ,  $l$ , and  $u$  into ‘‘point,’’ ‘‘line,’’ and ‘‘uniform’’ pieces. In the point piece one of the  $q$ 's has value unity, and the other two are zero. In the line piece one of the  $q$ 's is set to zero, and the other two are determined as in the  $N=2$  uniform distribution. Finally, the particles in the uniform piece have their  $q$ 's determined exactly as in the  $N=3$  uniform distribution. Our numerical data for the spheres are consistent with the values  $p=0.017\pm 0.0023$ ,  $l=0.1635\pm 0.007$ ,  $u=1-l-p=0.8195\pm 0.007$ .

We now discuss our results for the distribution of vertical forces. First, we calculated the force distribution at several different depths  $D$ . Our numerical data indicate that if one considers the normalized force  $v=w/D$ , the force distribution  $P(v)$  indeed becomes independent of depth for  $D\gtrsim 5$ , and it decays exponentially at large  $v$ . The data were obtained by making a histogram of the vertical force exerted by spheres in horizontal slices of width  $\Delta D=1$ . The scales are set by the normalization requirements  $\int_0^\infty dv v P(v)=1$ ,  $\int_0^\infty dv v P(v)=1$ .

We now compare the results of these molecular dynamics simulations to results from the  $q$  model. Figure 7 shows  $P(v)$  calculated via numerical simulation of the  $q$  model Eq. (2.1) with  $f(q)=1$  at depth  $D=1024$  on a periodically continued fcc lattice of side 1024, with  $N=3$ . Within our approximation of placing the grains on a uniform lattice, the reasonable choice for  $N$  is the dimensionality  $d$  of the system: For  $d=3$  the grains are approximated as being in triangular lattice layers, with each layer staggered relative to the next, so that each grain has three neighbors. As expected, since the mean field distribution is exact for the uniform case, there is excellent agreement with Eq. (2.24). On the same graph we show  $P(v)$  obtained in the sphere simulation described above. Both the sphere simulation and the  $q$  model exhibit a  $P(v)$  that decays exponentially at large  $v$ . The quantitative agreement between the two is surprisingly good considering the ‘‘arching’’ [1] in the sphere simulation, as reflected in the line and point pieces of the  $q$  distribution for the spheres. To examine the effects of arching on the results, we examined the force distribution resulting from the ‘‘ $q$  model’’ with the three-piece  $q$  distribution, which more closely approximates that of the sphere simulation. Figure 8 shows the numerically calculated  $P(v)$  for the  $q$  model with the three-piece distribution with  $p=0.017$  and  $l=0.1635$ , together with the solution for the uniform distribution and the numerical data from the sphere simulation. Changing the  $q$  distribution has little effect on  $P(v)$ ; to the extent that there is a change, it appears to improve the already good agreement between the  $q$  model and the sphere simulation.

Thus, our simulations indicate that our sphere packings are reasonably well-described (at the  $\sim 15\%$  level) by the uniform  $q$  distribution. Deviations from this  $q$  distribution are observed; accounting for them improves the already good agreement between the  $q$  model and the simulations.

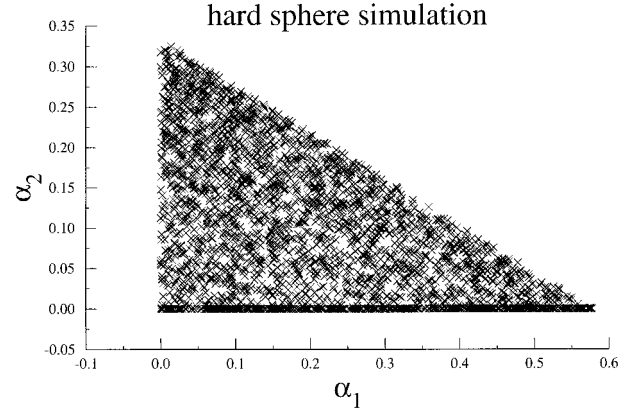


FIG. 6. Scatter plot of contact variables  $\alpha_1$ ,  $\alpha_2$  (defined in the text) obtained from the sphere simulation described in the text. The graph has 3229 points. On this plot, the uniform  $q$  distribution would have a uniform density of points. The ‘‘arching’’ in the simulation is reflected in the fact that a nonzero fraction of points have  $\alpha_2=0$ .

#### IV. DISCUSSION

This paper presents a statistical model for the force inhomogeneities in static bead packs and compares the results to numerical simulations of disordered sphere packings. The irregularities of the packing are described probabilistically, in terms of spatially uncorrelated random variables. Although there is a special  $q$  distribution for the  $q$  model that leads to a force distribution that decays as a power law at large forces, we have presented evidence that the force distribution decays exponentially at large forces for almost all  $q$  distributions. We obtain exact results for all the multipoint force correlation functions at a given depth for a countable set of  $q$  distributions, including one that is ‘‘generic’’ (the ‘‘uniform’’ distribution). The force distribution function for the uniform case agrees quantitatively with that obtained for the sphere simulation. Our numerical calculations demonstrate that a modified distribution of  $q$ 's which more closely approximates that observed for the sphere simulation improves the already good agreement between the force distribution predicted by the  $q$  model using the uniform  $q$  distribution and simulations of spheres. Thus, this model appears to contain some essential features of the force inhomogeneities in granular solids.

Neither our simulations nor the  $q$  model of Eq. (2.1) captures all features of real bead packs. In our simulations, we have included only central forces and have ignored friction; the  $q$  model ignores the vector nature of the forces, assuming that only the component along the direction of gravity plays a vital role. The qualitative consistency between the results obtained using the different methods as well as with experiment [6] provides some indication that the effects that we have neglected do not determine the main qualitative features of the force distribution at large  $v$ .

Several avenues for future investigations are evident. It should be straightforward to extend the analysis of the model to calculate longitudinal (along the direction of gravity) correlations of the forces. It is not obvious how to measure these correlations experimentally, but comparison to sphere simulations is clearly possible and would provide further tests of

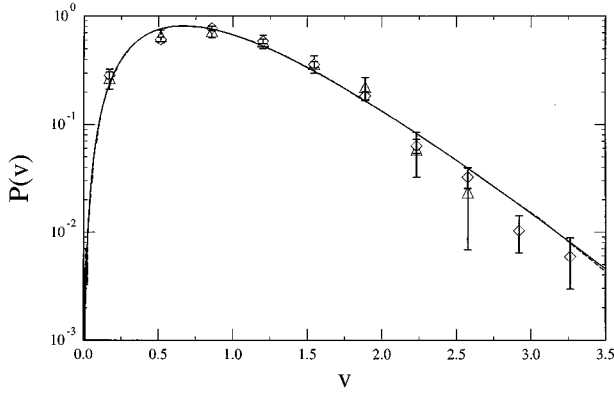


FIG. 7. The distribution of forces  $P(v)$  as a function of normalized weight  $v=w/D$  at a given depth  $D$ . Dashed line:  $P(v)$  at  $D=1024$  obtained via numerical simulation of the model Eq. (2.1) with  $f(q)=1$  on a periodically continued fcc lattice of transverse extent 1024. Solid line:  $P_u(v)$  obtained from the analytic mean field solution, Eq. (2.24). The points are  $P(v)$  obtained in the sphere simulation described in the text at depth  $D=10$  (triangles) and averaged over depths  $D=6$  through  $D=13$  (diamonds). There are no adjustable parameters; the scales are set by the normalization requirements  $\int_0^\infty dv P(v)=1$ ,  $\int_0^\infty dv vP(v)=1$ .

the statistical model. Similarly, the theory makes clearcut predictions for the multipoint correlation functions, which can be tested both by experiment and by simulations. The model can be generalized to apply to a broader variety of situations by including vector forces as well as incorporating boundary effects. Most interestingly, we plan to investigate whether the statistical theory developed here can be extended to provide new insight into the complex dynamical effects exhibited by granular materials [1].

In summary, we have presented and analyzed a statistical model for force inhomogeneities in stationary bead packs. The model, which predicts that force inhomogeneities decay exponentially at large forces for almost all contact distributions, agrees well with numerical simulations of sphere packings as well as experiment [6].

#### ACKNOWLEDGMENTS

We thank S. Nagel for many useful conversations as well as collaboration and A. Pavlovitch for discussions and for providing us with Ref. [26] prior to publication. O.N. acknowledges support from Harvard University and the Institute for Theoretical Physics at Santa Barbara (NSF Grant No. PHY89-04035). This work was supported in part by the MRSEC Program of the National Science Foundation under Contract Nos. DMR-8819860 and DMR-9400379.

#### APPENDIX: UNIFORM $q$ DISTRIBUTION

Here we consider the ‘‘uniform’’  $q$  distribution, which is the simplest  $q$  distribution consistent with the restriction that  $\sum_{i=1}^N q_i=1$ . It is obtained by choosing each of  $q_1, q_2, \dots, q_{N-1}$  independently from a uniform distribution between 0 and 1, setting  $q_N=1-\sum_{j=1}^{N-1} q_j$ , and then keeping only those sets where  $q_N \geq 0$ . Here we show that  $\eta_u(q)=1/(N-1)(1-q)^{N-2}$  for this distribution.

For  $N=2$ , if one chooses  $q_1$  between 0 and 1, then  $q_2=1-q_1$  must also be between 0 and 1, so that  $\eta_u(q)=1$ .

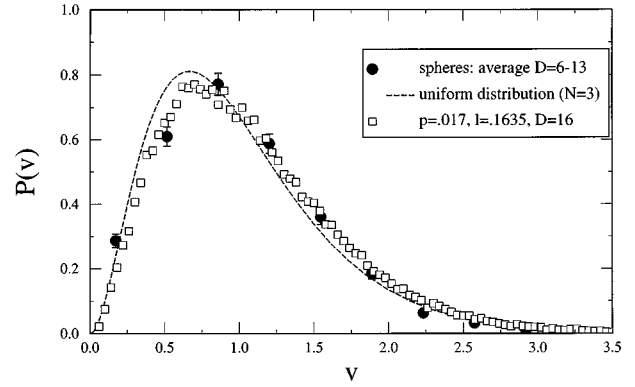


FIG. 8. The distribution of forces  $P(v)$  as a function of normalized weight  $v=w/D$  at a given depth  $D$ . Dashed line:  $P_u(v)$  obtained from the analytic mean field solution for  $q$  model with  $N=3$ , Eq. (2.24). Solid circles:  $P(v)$  obtained in the sphere simulation averaged over depths  $D=6$  through  $D=13$ . Open squares:  $P(v)$  at  $D=16$  obtained via numerical simulation of the model Eq. (2.1) with the three-part  $q$  distribution described in the text, with parameter values given on the graph, on a periodically continued fcc lattice of transverse extent 256. This figure demonstrates that using the measured  $q$  distribution instead of the uniform  $q$  distribution improves the already good agreement between the  $q$  model and the sphere simulation.

When  $N=3$ , configuration will be retained only if  $q_1+q_2+q_3 \leq 1$ . Therefore, the probability of obtaining a value of  $q$  is given by

$$\begin{aligned} \eta_u(q) &= M \int_0^1 dq_1 \int_0^1 dq_2 \delta(1-q_1-q_2-q) \\ &= M \int_0^{1-q} dq_1 = M(1-q), \end{aligned} \quad (\text{A1})$$

where  $M$  is a normalization constant. Since  $\int_0^1 dq \eta(q)=1$ , one immediately finds  $M=2=(N-1)$ .

For general  $N$ ,  $\eta_u(q)$  can be written:

$$\eta_u(q) = V(q) / \int_0^1 V(q) dq, \quad (\text{A2})$$

where

$$\begin{aligned} V(q) &= \int_0^1 dq_2 \int_0^{1-q_2} dq_3 \cdots \int_0^{1-\sum_{i=1}^{N-1} q_i} dq_n \\ &\quad \times \delta\left(1-q-\sum_{i=2}^N q_i\right). \end{aligned} \quad (\text{A3})$$

Using the identity

$$\begin{aligned} &\int_0^{1-\sum_{j=1}^{n-k} q_m} \left(1-\sum_{m=1}^{n-k+1} q_m\right)^{k-1} dq_{n-k+1} \\ &= \frac{1}{k} \left(1-\sum_{m=1}^{n-k} q_m\right)^k, \end{aligned} \quad (\text{A4})$$

one can show that

$$\eta_N(q) = (N-1)(1-q)^{N-2}. \quad (\text{A5})$$

- [1] See, e.g., H. M. Jaeger, J. B. Knight, C.-h. Liu, and S. R. Nagel, *Mat. Res. Soc. Bull.* **19**, 25 (1994); H. M. Jaeger and S. R. Nagel, *Science* **255**, 1523 (1992); *Disorder and Granular Media*, edited by D. Bideau and A. Hansen (North-Holland, Amsterdam, 1993); *Powder and Grains 93*, edited by C. Thornton (A. A. Balkema, Rotterdam, 1993); *Granular Matter*, edited by A. Mehta (Springer, Berlin, 1993).
- [2] See, e.g., J. D. Bernal, *Proc. R. Soc. London A* **280**, 299 (1964).
- [3] P. Dantu, *Ann. Ponts Chaussees IV*, 144 (1967); A. Drescher and G. de Josselin de Jong, *J. Mech. Phys. Solids* **20**, 337 (1972); T. Travers, M. Ammi, D. Bideau, A. Gervois, J. C. Messenger, and J. P. Troadec, *Europhys. Lett.* **4**, 329 (1987).
- [4] S. B. Savage, *Adv. Appl. Mech.* **24**, 289 (1984); R. M. Nedderman, U. Tuzun, S. B. Savage, and G. T. Houlsby, *Chem. Eng. Sci.* **37**, 1597 (1982); C. S. Campbell, *Annu. Rev. Fluid Mech.* **22**, 57 (1990).
- [5] C.-h. Liu and S. R. Nagel, *Phys. Rev. Lett.* **68**, 2301 (1992); *Phys. Rev. B* **48**, 15 646 (1993); C.-h. Liu, *ibid.* **50**, 782 (1994).
- [6] C.-h. Liu *et al.*, *Science* **269**, 513 (1995).
- [7] See, e.g., B. Mandelbrot, *The Fractal Geometry of Nature* (Freeman, San Francisco, 1983).
- [8] H. Takayasu and I. Nishikawa, in *Proceedings of the 1st International Symposium for Science on Form*, edited by S. Ishizaka (KTK, Tokyo, 1986), p. 15.
- [9] A. E. Scheidegger, *Bull. Intl. Acco. Sci. Hydrol.* **12**, 15 (1967).
- [10] H. Takayasu, I. Nishikawa, and H. Tasaki, *Phys. Rev. A* **37**, 3110 (1988).
- [11] G. Huber, *Physica* **170A**, 463 (1991).
- [12] D. Dhar and R. Ramaswamy, *Phys. Rev. Lett.* **63**, 1659 (1989).
- [13] S. N. Majumdar and C. Sire, *Phys. Rev. Lett.* **71**, 3729 (1993).
- [14] D. Dhar (unpublished).
- [15] The use of the term “sandpile” in this context is rather unfortunate, since we are exploiting a mathematical equivalence and do not suggest that the dynamical properties of models of SOC are directly related to the static properties of bead packs.
- [16] P. Bak *et al.*, *Phys. Rev. Lett.* **59**, 381 (1987).
- [17] The claim that  $P_D(v)$  becomes independent of  $D$  as  $D \rightarrow \infty$  is supported by the results of numerical simulations as well as by the fact that we obtain a consistent analytic solution for the distribution  $P_{D \rightarrow \infty}(v)$ .
- [18] Note that in the  $q_{0,1}$  limit, Eq. (2.11) has a singular solution,  $\tilde{P}(s)=1$ , that disagrees with the exact results. This is because [as can be seen by doing a similar mean field analysis in the  $q_{0,1}$  limit in terms of  $Q_D(w)$ ] the terms proportional to  $1/D$  dropped in going from Eq. (2.10) to Eq. (2.11) are important for the critical case. This is reasonable physically; for a critical system, although the injection process becomes less and less important in terms of the normalized variables as  $D \rightarrow \infty$ , the “relaxation time” [the number of levels one must propagate downwards before a perturbation  $\delta P(v)$  decays away] diverges, so that  $P(v)$  never settles to an equilibrium form, and the injection cannot be ignored. No such complications are expected away from criticality, where the relaxation time should be finite.
- [19] Some  $\rho(q_1, \dots, q_N)$  that are not of product form induce  $\eta(q)$ 's which have  $\delta$  functions at  $q=0$  and not at  $q=1$  (but not vice versa).
- [20] See, e.g., A. Katz, *Principles of Statistical Mechanics: The Information Theory Approach* (Freeman, San Francisco, 1967).
- [21] L. Rothenburg, Ph.D. thesis, Carleton University, Ottawa, Canada, 1980.
- [22] J. Zinn-Justin, *Quantum Field Theory and Critical Phenomena* (Clarendon, Oxford, 1990), p. 214 [Eq. (9.39)]; P. Ramond, *Field Theory: A Modern Primer* (Benjamin-Cummings, Reading, MA, 1981), p. 157 [Eq. (4.8)].
- [23] P. A. Cundall, J. T. Jenkins, and I. Ishibashi, in *Powders and Grains*, edited by J. Biarez and R. Gourves (Balkema, Rotterdam, 1989), pp. 319–322.
- [24] J. T. Jenkins, P. A. Cundall, and I. Ishibashi, in *Powders and Grains* (Ref. [23]), pp. 257–274.
- [25] K. Bagi, in *Powders and Grains* (Ref. [1]), pp. 117–121.
- [26] A. Pavlovitch (unpublished).
- [27] For beads with more than three contacts, say,  $f_1, f_2, f_3$ , and  $f_4$ , only the three strongest contacts were picked and renormalized to derive the  $q$ 's, namely,  $q_1 = f_1 / (f_1 + f_2 + f_3)$ , etc.
- [28] The  $q$ 's are related to the  $\alpha$ 's via  $q_1 = \alpha_2$ ,  $q_2 = \frac{1}{2}(1 - \sqrt{3}\alpha_1 - \alpha_2)$ ,  $q_3 = \frac{1}{2}(1 + \sqrt{3}\alpha_1 - \alpha_2)$ .